J. Mech. Phys. Solids 180 (2023) 105423

Contents lists available at ScienceDirect

Journal of the Mechanics and Physics of Solids

journal homepage: www.elsevier.com/locate/jmps

The fibrous character of pericellular matrix mediates cell mechanotransduction

Xiangjun Peng, Yuxuan Huang, Guy M. Genin *

U.S. National Science Foundation Science and Technology Center for Engineering Mechanobiology, and Department of Biomedical Engineering, Washington University, St. Louis, MO 63130 United States

ARTICLE INFO

Keywords:
Cell contractility
Pericellular matrix
Mechanical signaling
Mechanobiology

ABSTRACT

Cells in solid tissues sense and respond to mechanical signals that are transmitted through extracellular matrix (ECM) over distances that are many times their size. This long-range force transmission is known to arise from strain-stiffening and buckling in the collagen fiber ECM network, but must also pass through the denser pericellular matrix (PCM) that cells form by secreting and compacting nearby collagen. However, the role of the PCM in the transmission of mechanical signals is still unclear. We therefore studied an idealized computational model of cells embedded within fibrous collagen ECM and PCM. Our results suggest that the smaller network pore sizes associated with PCM attenuates tension-driven collagen-fiber alignment, undermining long-range force transmission and shielding cells from mechanical stress. However, elongation of the cell body or anisotropic cell contraction can compensate for these effects to enable long distance force transmission. Results are consistent with recent experiments that highlight an effect of PCM on shielding cells from high stresses. Results have implications for the transmission of mechanical signaling in development, wound healing, and fibrosis.

1. Introduction

Animal cells commonly reside within a three-dimensional (3D) fibrous extracellular matrix (ECM), to which they attach via cell surface proteins such as integrins (Hall et al., 2016). External mechanical stimuli can be transmitted through ECM fibers to these surface proteins, and then on to the cytoskeleton and cell nucleus to affect gene expression (Alisafaei et al., 2023; Huang et al., 2017; Rashid et al., 2023; Romani et al., 2021). The cell itself can generate contraction through molecular motors such as myosins to stretch and remodel fibrous ECM (Hall et al., 2016). These interactions between the cells and ECM affect many physiological and pathological processes, including wound healing (Shakiba et al., 2020), fibrosis (Liu et al., 2020; Long et al., 2022), and cell proliferation (Saraswathibhatla et al., 2023).

Collagen, the most abundant ECM protein in the body, forms dense fibrous tissues, but presents as a sparser network earlier in development and in healing. When loaded by mechanical forces arising from cells or from outside of the tissue, collagen networks can align (Alisafaei et al., 2021), stiffen (Hall et al., 2016; Wang et al., 2014), and undergo plastic deformation (Ban et al., 2018). As cells adapt their local environment, they can secrete, digest and recruit collagen in the "pericellular" region around the cell body, leading to a region of pericellular matrix (PCM) with collagen concentration and stiffness exceeding those of the collagen more distal from the cell (Han et al., 2018; Liu et al., 2020; Shakiba et al., 2020). A relatively stiff PCM is known to shield chondrocytes from applied stress

* Corresponding author.
E-mail address: genin@wustl.edu (G.M. Genin).

https://doi.org/10.1016/j.jmps.2023.105423
Received 7 May 2023; Received in revised form 3 August 2023; Accepted 24 August 2023
Available online 27 August 2023

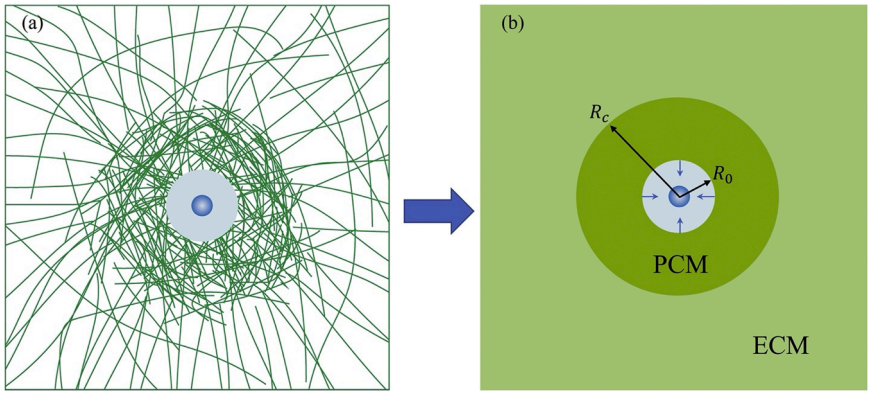

Fig. 1. (a) Schematic of a eukaryotic cell inside a collagen ECM with PCM. (b) The equivalent cell-matrix system, with the ECM and PCM represented by a fiber-inspired constitutive model.

(Alexopoulos et al., 2005), and its disruption can lead to significant pathology including cartilage degradation, osteoarthritis, and a shift in chondrocyte phenotype (Dowling et al., 2013; Reynolds et al., 2021). Stiffening of ECM and PCM by cells can occur through a number of mechanisms including alignment of collagen fibers (Ahmadzadeh et al., 2017), increases in collagen concentration (Doyle et al., 2015; Fraley et al., 2015), and thickening of fibers (Seo et al., 2020). The mechanical properties of fibrous ECM can be predicted from geometric parameters including the diameter and concentration of collagen fibers, (Alisafaei et al., 2022) and the distribution of pore sizes (Alisafaei et al., 2021; Ban et al., 2018; Hall et al., 2016; Wang et al., 2014).

ECM mechanics affects how cells remodel themselves and their microenvironment. Stiffening of collagen affects the stresses and strains experienced by cells, can lead cells to polarize along a major axis and stiffen (Ahmadzadeh et al., 2017; Alisafaei et al., 2022; Hall et al., 2016; Shakiba et al., 2020) and can eventually affect chemo-mechanical factors, gene expression, and cell differentiation (Han et al., 2016; Hong et al., 2022). Cell contractility increases with ECM stiffness and collagen concentration (Doyle et al., 2015; Fraley et al., 2015). Additionally, ECM remodeling affects communication between cells. Cells in fibrous matrix show long-range force sensing, that is, cells are capable of detecting and reacting to mechanical stimuli over distances that are several times their diameter (Alisafaei et al., 2021; Hall et al., 2016). These nonlinear properties of collagen enable cells to remodel the ECM and to engage in positive mechanical feedback between one another and the ECM (Hall et al., 2016). Remodeling affects not only the disposition of the PCM and ECM, but also the disposition of the cells themselves (Liu et al., 2020). However, the ways that the fibrous PCM and the associated spatial heterogeneity affect structure-function relationships and mechanical transduction across length scales remains poorly understood (Fang et al., 2014; Nerurkar et al., 2009).

From the mechanical point of view, microstructural heterogeneity clearly affects tissue mechanics, as seen from experiments such as ultrasound scattering by tissues (Peng et al., 2020a, 2020b) and observations of failure patterns in functionally graded tissues (Genin et al., 2009). Mechanical strain and stress transfer from tissues to cells in fibrocartilage is strongly heterogeneous (Han et al., 2016, 2013). Coatings around inclusions in a matrix can attenuate dynamic stress concentration (Peng et al., 2021) and enhance the mechanical properties of composite materials (Bonfoh et al., 2012). These phenomena inspired us to ask whether the existence microstructural heterogeneity from the PCM can also affect mechanosignaling.

To fill this gap in understanding how microstructural heterogeneity may contribute to micromechanics and mechanobiology, we developed a computational model that predicts how the fibrous PCM affects long-range force sensing. We first studied how the fibrous nature of the ECM and PCM affect force sensing, compared to linear elastic or linear hyperelastic ECM and PCM. We then quantitatively investigated how PCM properties, cell shape and polarization modulate the transmission of cell contractile forces. Finally, we evaluated how PCM affects the stresses transduced by cells in a far field stretch. We tested the hypotheses that the PCM attenuates long-range force transmission, cell-cell communication, and stress transfer to cells, and that the fibrous nature of the PCM accentuates this.

2. Methods

Model problem. To study the effects of the PCM on cell-level mechanotransduction, we modeled an axisymmetric, ellipsoidal, cell of semiminor axis R_0 and semimajor axis h. This was centered within an ellipsoidal region of PCM of outer semiminor axis length R_c that in turn was centered within a cylinder of a less dense, "far field" ECM (Fig. 1a). Periodic boundary conditions were applied, so that the normal displacements were constrained on the bottom surface of the cylinder, radial displacements were constrained to be identical at the outer boundary, and normal displacements were constrained to be identical at all points along the upper boundary. All other boundary conditions were traction free. The cylinder height was $20R_0$, and the thickness of the PCM was set to be $2R_0$ so that its outer boundary was at $R_c = 3R_0$.

To evaluate how the fibrous PCM affects force transmission, we compared predictions of displacement fields using several constitutive laws. The first, described below, is a continuum constitutive law that captures the fibrous nature of the ECM. This was compared to linear elastic and hyperelastic (neoHookean) constitutive models with initial elastic modulus and Poisson ratio matching that of the fibrous ECM constitutive model.

Cell contractility was modeled by a uniform contractile strain, as is appropriate for the early stages of cell spreading within a collagen ECM (Hall et al., 2016). A spherical eigenstrain tensor of magnitude 50% was applied to the PCM in the form of a displacement field on the inner boundary of the PCM.

Fiber network constitutive model. The fibrous mechanobiological environment in Fig. 1(a) was approximated by a network-inspired constitutive model (Fig. 1(b)) (Wang et al., 2014). As reported in the literature, collagen fiber networks show intrinsic properties that differ from those of a non-fibrous continuum. When an initially isotropic collagen network undergoes large strain, tension is carried disproportionately by a subset of fibers (Chen et al., 2022; Deogekar and Picu, 2018; Picu, 2011; Wang et al., 2014). Such fibers align into the direction of maximum principal strain and cause local stiffening, while fibers perpendicular to the direction of loading can buckle. This behavior is well approximated by a composite material of strain-aligning fibers in parallel with an isotropic background (Alisafaei et al., 2021; Hall et al., 2016; Wang et al., 2014). The total strain energy density W can be written as a sum of the contribution from aligned fibers, W_f, and that of the isotropic background fibers W_b (Alisafaei et al., 2021; Hall et al., 2016; Wang et al., 2014):

$$W = W_f + W_b \tag{1}$$

The isotropic contribution W_b from unaligned background fibers has been modeled by the neoHookean strain energy density function (Chen et al., 2022; Wang et al., 2014):

$$W_b = \frac{\mu}{2}(\bar{I}_1 - 3) + \frac{\kappa}{2}(J-1)^2 \tag{2}$$

where $\mu = E/(2(1+\nu))$ and $\kappa = E/(3(1-2\nu))$ are the initial shear and bulk modulus, respectively; E is the initial elastic modulus; and ν is the initial Poisson ratio. Here, the invariant J is defined as $J = \det(\mathbf{F})$, where $\mathbf{F}$ is the deformation gradient tensor with components $F_{ij} = \partial x_i/\partial X_j$, in which $\mathbf{x}$ and $\mathbf{X}$ represent points in the current and reference configurations, respectively. $\bar{I}_1 = J^{-\frac{2}{3}}(\lambda_1^2+\lambda_2^2+\lambda_3^2)$ is the is the first invariant of the deviatoric part the right Cauchy-Green deformation tensor, $\mathbf{C} = \mathbf{F}^{\mathbf{T}}\mathbf{F}$, where λ_1, λ_2, and λ_3 are the principal stretch ratios. $\mathbf{C}$ and the right Cauchy-Green deformation tensor $\mathbf{B} = \mathbf{F}\mathbf{F}^{\mathbf{T}}$ can be expressed via the spectral representations:

$$\mathbf{B} = \sum_{a=1}^{3} \lambda_a^2 \mathbf{n}_a \otimes \mathbf{n}_a \tag{3}$$

$$\mathbf{C} = \sum_{a=1}^{3} \lambda_a^2 \mathbf{N}_a \otimes \mathbf{N}_a \tag{4}$$

where $\mathbf{n}_a$ and $\mathbf{N}_a$ are the unit eigenvectors of $\mathbf{B}$ and $\mathbf{C}$, respectively.

To capture the strain-stiffening phenomenon of the fibrous ECM, (Hall et al., 2016) define the strain energy density contribution from the aligned fibers as:

$$W_f = \sum_{a=1}^{3} f(\lambda_a) \tag{5}$$

where $f(\lambda_a)$ is chosen to model the experimental observations that the collagen ECM stiffens only beyond a critical level of principal stretch, and that its energetic contribution vanishes if the critical value. To this end, the Cauchy stress tensor $\boldsymbol{\sigma} = \boldsymbol{\sigma}_{\mathbf{b}} + \boldsymbol{\sigma}_{\mathbf{f}}$ is decomposed into isotropic, $\boldsymbol{\sigma}_{\mathbf{b}}$, and stiffening, $\boldsymbol{\sigma}_{\mathbf{f}}$, contributions:

$$\boldsymbol{\sigma}_{\mathbf{b}} = \kappa(J-1)\mathbf{I} + \mu \mathrm{dev}(\overline{\mathbf{B}})/J \tag{6}$$

$$\boldsymbol{\sigma}_{\mathbf{f}} = \frac{1}{J}\sum_{a=1}^{3} \frac{\partial f(\lambda_a)}{\partial \lambda_a}\lambda_a(\mathbf{n}_{\mathbf{a}} \otimes \mathbf{n}_{\mathbf{a}}) \tag{7}$$

where $\mathbf{I}$ and $\overline{\mathbf{B}} = \mathbf{B}/J^{2/3}$ are the identity tensor and the left modified Cauchy-Green tensor, respectively, and Hall et al. (2016):

$$\frac{\partial f(\lambda_a)}{\partial \lambda_a} = \begin{cases} 0, & \delta\lambda_a < -\lambda_t \\ E_f \dfrac{(\delta\lambda_a + \lambda_t)^{n+2}}{\lambda_t^n (n+1)(n+2)}, & -\lambda_t \le \delta\lambda_a < 0 \\ E_f \left[\dfrac{(1+\delta\lambda_a)^{m+2}-1}{(m+1)(m+2)} - \dfrac{\delta\lambda_a}{m+1} + \dfrac{(\delta\lambda_a)\lambda_t}{n+1} + \dfrac{\lambda_t^2}{(n+1)(n+2)} \right], & \delta\lambda_a \ge 0 \end{cases} \tag{8}$$

in which $\delta\lambda_a = \lambda_a - (\lambda_c + 0.5\lambda_t)$, λ_c is the critical value of principal stretch for the transition to alignment-based stiffening, $\lambda_t = 0.5\lambda_c$ is the width of the transition range, the exponent n characterizes the increase in strain energy in the transition range, and the modulus E_f and strain-stiffening exponent m characterize stiffening due to collagen fiber alignment.

Solution procedures. We systematically evaluated the effects of PCM and the key material parameters on force transmission, cell mechanosensation, and strain shielding. For comparison, we also studied linear and nonlinear elastic ECM and PCM. Simulations were

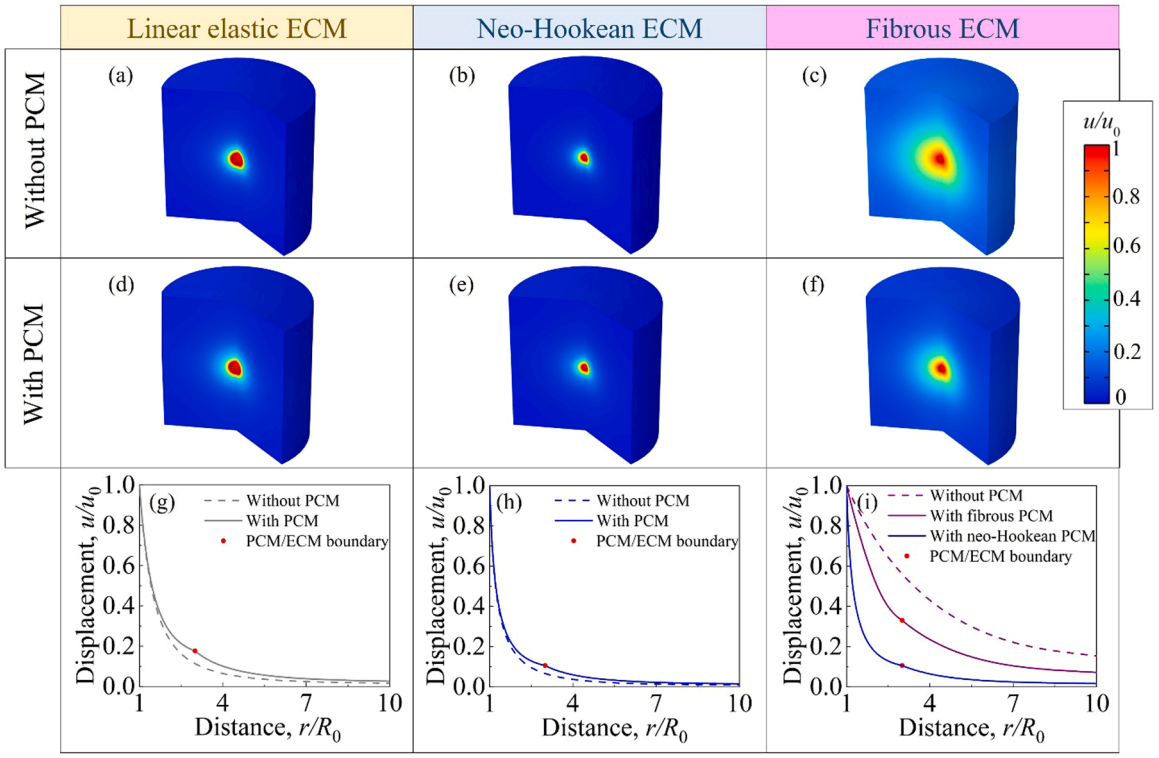

Fig. 2. The effect of PCM on displacement fields in 3D linear elastic, neoHookean, and fibrous ECMs when subjected to spherical and isotropic contraction from a cell. (a-c) Contour plots of normalized displacement fields due to cell contraction in systems with no PCM. (d-f) Contour plots illustrating the normalized displacement fields due to cell contraction in systems containing PCM. (g-i) Normalized displacement fields within the midplane of the cylinder. Included in panel *i* is the case of a neoHookean PCM surrounding a cell and embedded within a fibrous ECM. Parameters for all plots: E_{ECM}=2 kPa, E_{PCM}/E_{ECM}=100, Poisson's ratio $\nu = 0.3$; additionally, for the fibrous ECM: fiber stiffness $\chi_m = E_{fECM}/E_{ECM}$ =50, fiber strain-hardening exponent $m = 30$, critical stretch $\lambda_c = 1.001$. The thickness of the PCM was set to be $t = 2R_0$.

performed in the COMSOL environment (COMSOL, Inc., Burlington, MA). The nonlinear constitutive model was used, and finite deformation was modeled. To enter the fiber network constitutive model into COMSOL, the isotropic part of the Cauchy stress tensor $\boldsymbol{\sigma}_\mathbf{b}$ was obtained using the neoHookean constitutive model in COMSOL, while the stiffening contribution $\boldsymbol{\sigma}_\mathbf{f}$ was set as an external stress tensor. Because strain-stiffening attenuates with increasing collagen density due to reduced collagen reorientation in the direction of tension in matrix with lower pore size (Hall et al., 2016), the decomposed of the denser PCM into two families of collagen proceeded as follows. $\boldsymbol{\sigma}_\mathbf{b}$ for the PCM was associated with a modulus that was 100 times stiffer than that of the ECM, while the functions underlying $\boldsymbol{\sigma}_\mathbf{f}$ were set to be identical to those in the ECM.

Baseline parameters used in all simulations were the following. Initial elastic properties were $E_{ECM} = 2$ kPa (Babaei et al., 2016, 2017), $E_{PCM}/E_{ECM} = 100$ (Han et al., 2018), Poisson's ratio $\nu = 0.3$; additionally, for the fibrous ECM: fiber stiffness $\chi_m = E_{fECM}/E_{ECM} = 50$, fiber strain-hardening exponent $m = 30$, critical stretch $\lambda_c = 1.001$ (Hall et al., 2016; Wang et al., 2014). The thickness of the PCM was set to be $t = 2R_0$ (Shakiba et al., 2020).

3. Results and discussion

3.1. An elastic PCM accentuates force transmission, while a fibrous PCM attenuates it

As a comparison case, we first considered a contractile cell with no PCM (that is, with material parameters for the PCM set identical to those of the ECM), as studied by Wang et al. (2014). As expected from earlier studies (Alisafaei et al., 2021; Hall et al., 2016; Wang et al., 2014), displacement fields around cells embedded within linear elastic (Fig. 2a) or neoHookean (Fig. 2b) ECM decayed rapidly compared to displacement fields in fibrous ECM (Fig. 2c). Adding a relatively stiff, linear elastic or neoHookean PCM layer had moderate effects on displacement fields in linear elastic (Fig. 2d) and neoHookean (Fig. 2e) ECM, but much greater and diametrically opposite effects in fibrous PCM and ECM (Fig. 2f).

These trends are evident in plots of the normalized displacement u/u_0 versus the normalized distance r/R_0 along the midplane of the cylinder. As expound upon by Wang et al. (Wang et al., 2014), in the absence of PCM, displacement decays in a linear elastic ECM following the $1/r^2$ scaling of the Eshelby solution (Fig. 2g). In a neoHookean ECM, the decay is more rapid still (Fig. 2h). On the contrary, the scaling in a fibrous ECM is much slower (Fig. 2i), less than $1/r$, which indicates that force transmission is long-range.

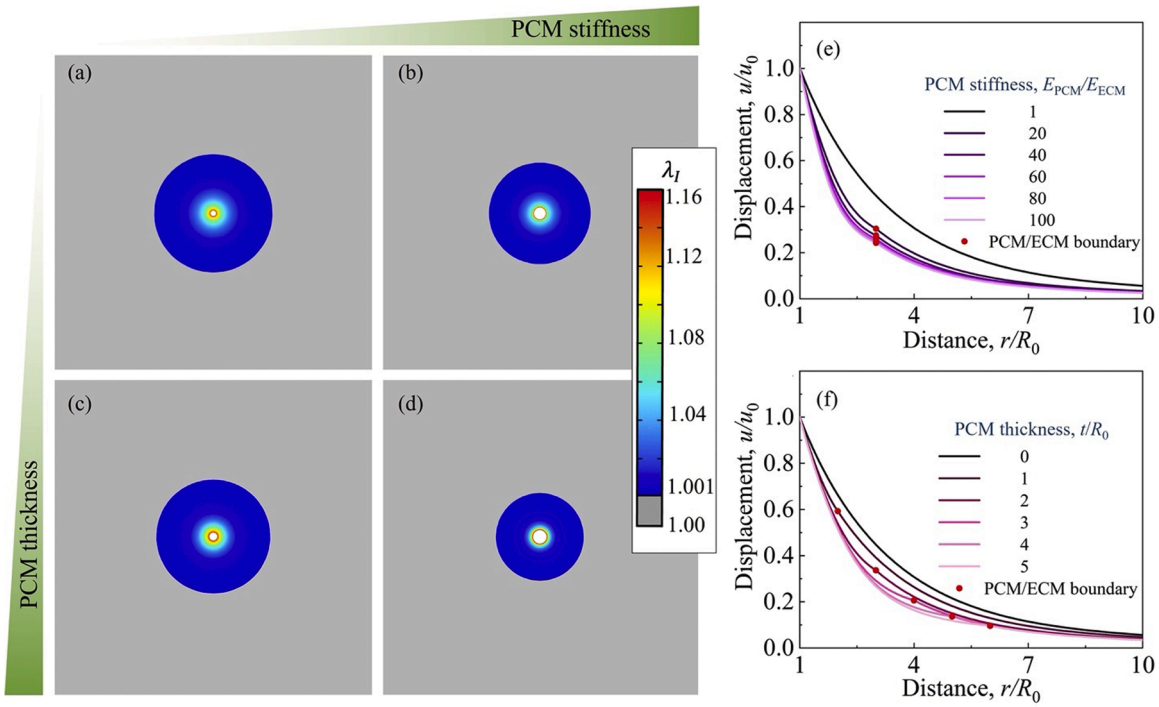

Fig. 3. Effects of PCM thickness and stiffness on force transmission in 3D fibrous medium. (a-d) Contour plots displaying aligned regions in color and isotropic regions in gray regions for four cases. (e-f) Normalized radial displacement u/u_0 versus normalized distance r/R_0 with PCM of different PCM stiffness and thickness. Parameters for all plots: $E_{ECM} = 2$ kPa, $E_{PCM}/E_{ECM} = 100$, Poisson's ratio $\nu = 0.3$; additionally, for the fibrous ECM: fiber stiffness$\chi_m = E_{fECM}/E_{ECM} = 50$, fiber strain-hardening exponent $m = 30$, critical stretch $\lambda_c = 1.001$.

Addition of PCM had opposite effects in fibrous and non-fibrous systems. In a linear elastic or neoHookean system, the decay of displacement was attenuated by the PCM (Fig. 2g-h), but in a fibrous system decay was accelerated by the PCM (Fig. 2i). In the linear elastic and neoHookean systems, because the PCM elastic modulus E_{PCM} is larger than that of the ECM, E_{ECM}, the boundary displacement u_0 is transmitted through the PCM to reach the PCM-ECM boundary, leading to larger deformation relative to what would occur in the absence of PCM (Fig. 2g-h). However, for the fibrous ECM, due to strain-stiffening, the relatively stiff PCM has the opposite effect. The smaller pore size of the PCM reduces the collagen network reorientation underlying strain-stiffening, and thus reduces the associated long-range force transmission. The decay in displacement thus accelerates towards that observed in linear elastic and neoHookean systems (Fig. 2i). However, the fibrous system does retain greater long-range force transmission capacity than the other two systems because even in the relatively dense, fibrous PCM, the collagen network can still realign and strain-stiffen in response to stretch.

The mechanics of the matrix material directly surrounding cells is not as well characterized as that of more distal ECM. A possibility is that the material in the direct vicinity of the cell membrane, including recently synthesized collagen, is not fully fibrous in character (Siadat and Ruberti, 2023). To assess how this might affect mechanical communication between cells, we studied cells with a non-fibrous PCM, represented by a neoHookean material, embedded within a fibrous ECM. In this case, as expected because of the absence of strain-stiffening, the displacement field attenuates within the neoHookean PCM at a rate that is substantially faster than attenuation within a fibrous PCM, with relatively little displacement reaching the fibrous outer ECM (Fig. 2i).

The analyses described above were performed with cell contractility modeled as an inward displacement of the PCM. However, contractility of cells within more highly remodeled PCM may instead be more consistent with an applied traction. To explore this, a traction of 0.4 kPa (Zahalak et al., 2000) was applied on the inner boundary of the PCM, with all other parameters identical to those of the simulations reported in Fig. 2. Once again, the effect of the PCM on the decay of displacement through a fibrous ECM was opposite the effect of the PCM on the decay of displacement through a linear elastic or neoHookean ECM (Fig. A1). These results further highlight the role of a fibrous ECM in enabling long-range force transmission, and in enabling stress shielding by cells via effects of the PCM.

3.2. *Effects of PCM stiffness and PCM thickness on force transmission in 3D matrices*

Both the PCM stiffness, E_{PCM}/E_{ECM}, and the PCM thickness, t/R_0, can affect long-range force transmission (Fig. 3). Here, we focused only on the case of a fibrous ECM. The contour plots of Fig. 3, which show the first principal stretch λ_I beginning with levels that exceed the critical stretch $\lambda_c = 1.001$, reveal that increasing the PCM stiffness (Fig. 3b) or PCM thickness (Fig. 3c) attenuates force

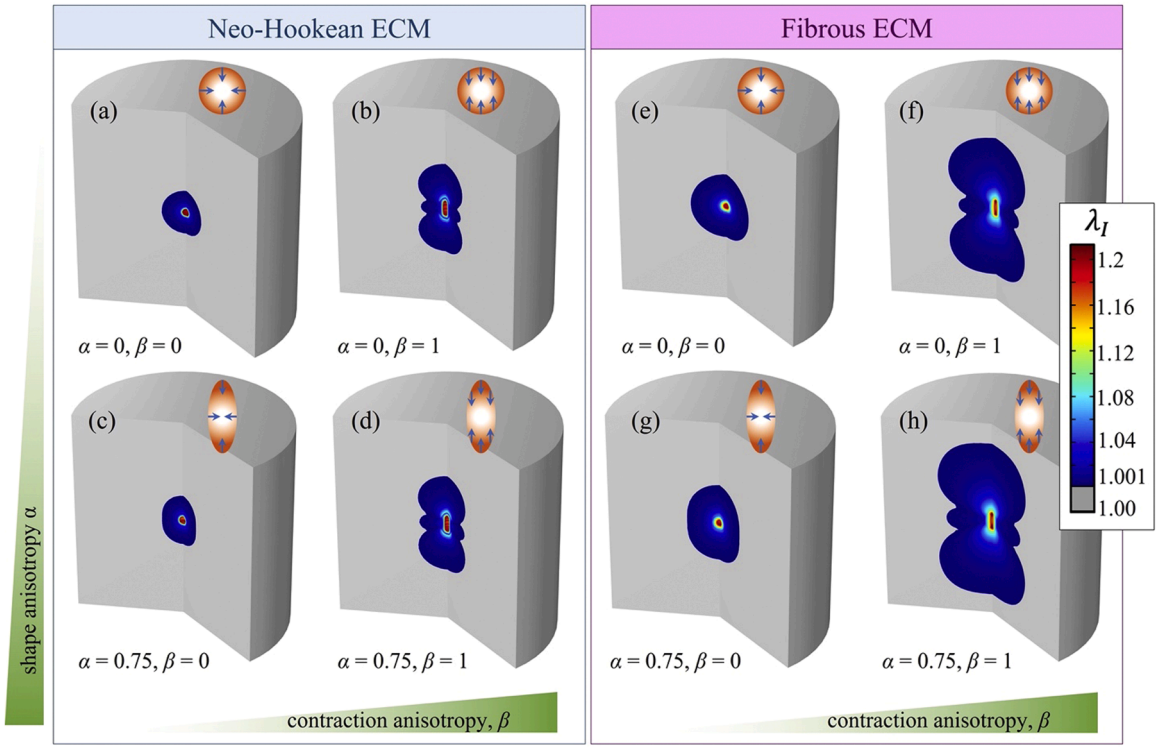

Fig. 4. Effects of shape and contraction anisotropies of cells on strain fields in neoHookean and fibrous PCM and ECM. (a-d) Contour plots of first principal stretch in neoHookean ECM and PCM. (e-h) Contour plots of first principal stretch in fibrous ECM and PCM. Parameters for all plots: $E_{ECM} = 2$ kPa, $E_{PCM}/E_{ECM} = 100$, Poisson's ratio $\nu = 0.3$; additionally, for the fibrous system: fiber stiffness $\chi_m = E_{fECM}/E_{ECM} = 50$, fiber strain-hardening exponent $m = 30$, critical stretch $\lambda_c = 1.001$. The thickness of the PCM was set to be $t = 2R_0$.

transmission. The impact is amplified when both factors are increased at the same time (Fig. 3d).

For better comparison, we again plotted the normalized displacement u/u_0 versus the normalized distance r/R_0 (Fig. 3e-f). Keeping the PCM thickness constant at $t = 2R_0$ and increasing the PCM stiffness E_{PCM}/E_{ECM} increased the rate of decay of u/u_0 up to a limit of $E_{PCM}/E_{ECM} \approx 80$ (Fig. 3e). This trend is expected because larger PCM stiffness E_{PCM}/E_{ECM} means smaller collagen network pores and less collagen realignment and strain-stiffening. Keeping the PCM stiffness at $E_{PCM} = 10E_{ECM}$ and varying the PCM thickness also affected force transmission (Fig. 3f). Note that the PCM/ECM boundary (circular symbol in Fig. 3f, red online) shifted in each case illustrated. Increasing the PCM thickness increased the rate of decay of the normalized displacement field, especially within PCM itself (Fig. 3f). This trend is also expected because force transmission is attenuated within the denser PCM.

3.3. Cell shape and polarization affect force transmission through fibrous PCM

As cells such as fibroblasts adapt to their extracellular environment, they develop polarity in their shape, shifting from spherical to spindle-shaped, and in the direction in which they apply contractile force, eventually developing contraction along the long axis (Alisafaei et al., 2019; Hall et al., 2016; Shakiba et al., 2020). To study the effect of polarization in shape, we model cells as prolate spheroids by $(x/R_0)^2 + (y/R_0)^2 + (z/h)^2 \leq 1$ (Fig. 4). To study shape parametrically, a shape index $\alpha = 1 - R_0/h$ was defined, with $\alpha = 0$ corresponding to a sphere and $\alpha \to 1$ corresponding to a highly elongated, prolate spheroid. To study the effect of polarization in contractility, we imposed a compressive strain (stretch ratio $\lambda_z^{cell} < 1$) along the semimajor axis of the cell and a lesser, equibiaxial compressive strain ($\lambda_x^{cell} = \lambda_y^{cell} \equiv \lambda_\perp^{cell}$) along the semiminor axes. To study this parametrically, a polarization ratio $\beta = (1 - \lambda_\perp^{cell}/\lambda_z^{cell})/(1 - J^{cell})$ was defined, in which the Jacobian $J^{cell} = (\lambda_\perp^{cell})^2 \lambda_z^{cell}$ was maintained at 0.5 over all simulations to enable comparisons. Note that $\beta = 0$ represents a cell contracting isotropically, whereas $\beta = 1$ represents uniaxial contraction along the major axis.

Force transmission in fibrous matrices was impacted by both the anisotropy of contraction and shape. (Fig. 4). Contours of ECM and PCM principal stretch ratios that exceeded the critical stretch, λ_c, revealed different effects of the PCM on force transmission through fibrous and neoHookean ECM with PCM of similar thickness (Fig. 4). In all cases, mechanical signals traveled further through a fibrous system. Shape and contractile anisotropy both led to an expanded region of fiber alignment in a fibrous system, and the effect was more pronounced when both factors were present at the same time (Fig. 4h). This is expected because both the shape and contraction anisotropy concentrate tensile strains in the longitudinal orientation of the cells, and extended regions of fiber alignment thus arise from the concentrated tensile strains associated with this synergy. Thus, although a fibrous PCM attenuates force transmission, changes

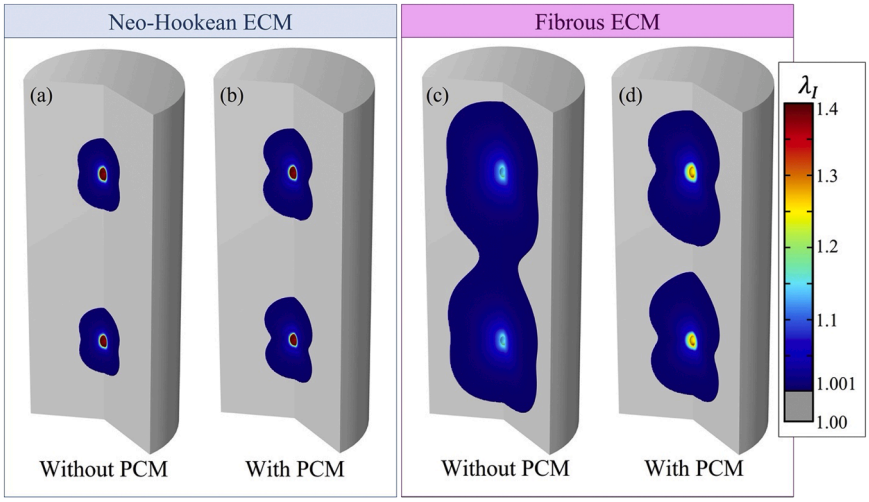

Fig. 5. Interactions of two contractile cells (sphericity index α=0.5, polarization ratio $\beta = 0$) in a 3D neoHookean (a-b) and fibrous ECM (c-d) with or without PCM. Parameters for all plots: $E_{ECM} = 2$ kPa, $E_{PCM}/E_{ECM} = 100$, Poisson's ratio $\nu = 0.3$; additionally, for the fibrous system: fiber stiffness$\chi_m = E_{fECM}/E_{ECM} = 50$, fiber strain-hardening exponent $m = 30$, critical stretch $\lambda_c = 1.001$, PCM thickness $t = 2R_0$.

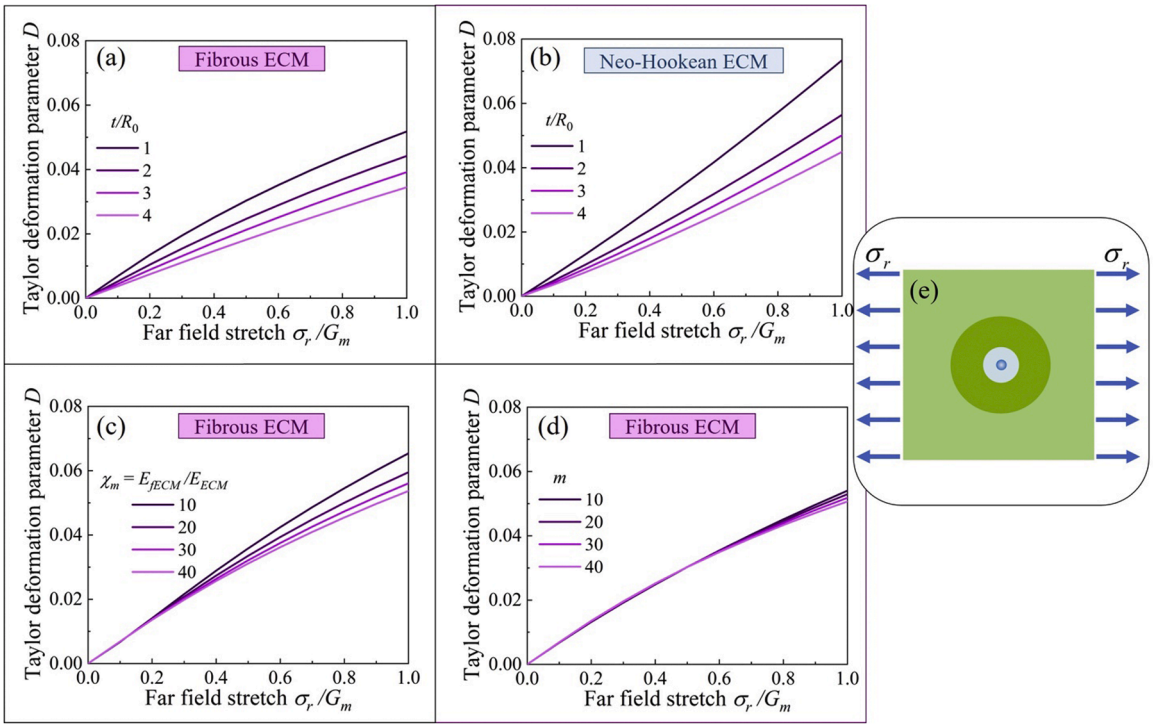

Fig. 6. Cell stretch as a function of normalized far field stretch σ_r/G_m for a spherical cell embedded in a 3D PCM and ECM, as characterized by the Taylor deformation parameter, D. (a) Effect of PCM thickness for a cell in fibrous system. (b) Effect of PCM thickness for a cell in a neoHookean system. (c) Effect of fiber stiffness χ_m for a cell in a fibrous system. (d) Effect of fiber strain-hardening exponent, m, for a cell in a fibrous system. (e) Schematic of model problem. Baseline parameters for all plots: $E_{ECM} = 2$ kPa, $E_{PCM}/E_{ECM} = 100$, Poisson's ratio $\nu = 0.3$; additionally, for the fibrous system: fiber stiffness$\chi_m = E_{fECM}/E_{ECM} = 50$, fiber strain-hardening exponent $m = 30$, critical stretch $\lambda_c = 1.001$, PCM thickness $t = 2R_0$.

in cell shape and contractile polarity can counteract this attenuation.

3.4. A fibrous PCM interferes with mechanical communication between cells

To examine how attenuation force transmission by the PCM may also impact the cell sensing interactions that are essential to

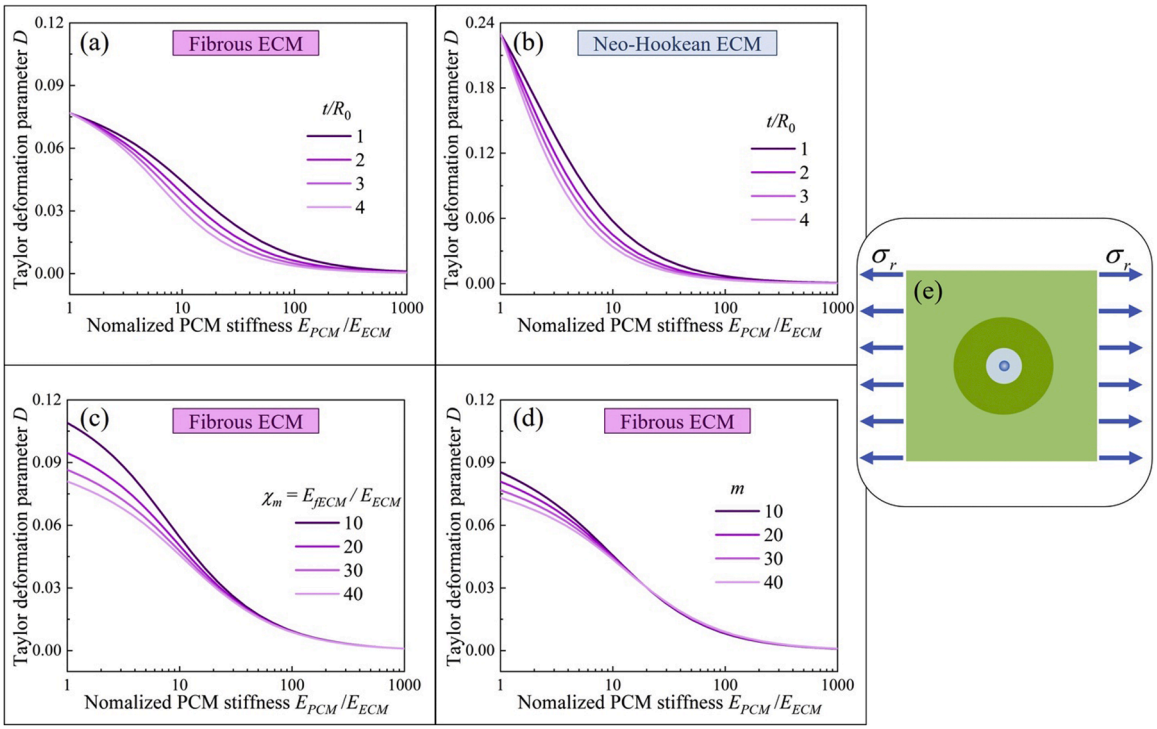

Fig. 7. Cell stretch, as characterized by the Taylor deformation parameter, D, as a function of PCM stiffness for a cell embedded in a 3D PCM and ECM that is loaded uniaxially with a far field stretch σ_r/G_m=0.5. (a) Effects of PCM thickness for a cell in fibrous system. (b) Effects of PCM thickness for a cell in a neoHookean system. (c) Effect of fiber stiffness χ_m for a cell in a fibrous system. (d) Effect of fiber strain-hardening exponent, m, for a cell in a fibrous system. (e) Schematic of model problem. Baseline parameters for all plots: $E_{ECM} = 2$ kPa, $E_{PCM}/E_{ECM} = 100$, Poisson's ratio $\nu = 0.3$; additionally, for the fibrous system: fiber stiffness$\chi_m = E_{fECM}/E_{ECM} = 50$, fiber strain-hardening exponent $m = 30$, critical stretch $\lambda_c = 1.001$, PCM thickness $t = 2R_0$.

morphogenesis, wound healing, and fibrosis, we simulated how two cells would interact in both 3D fibrous and neoHookean matrices (Fig. 5). Cells were spaced a distance of $50R_0$ and given a sphericity index of α=0.5 and a polarization ratio of $\beta = 0$. As in previous simulations, the PCM thickness was set to $t = 2R_0$ and isotropic modulus set to $E_{PCM} = 100E_{ECM}$.

In a neoHookean ECM, strain decayed substantially before the lowest principal stretch contour ($\lambda_I = \lambda_c$) was reached, regardless of the presence or absence of PCM (Fig. 5a-b). In a fibrous system, recruitment of fibers extended into the matrix so that significant overlap of regions of fiber alignment between the two cells extended a distance of 20 times the cell radius. PCM attenuated this, with the overlap to vanishing and cells less unable to transduce mechanical signals from one other. Again, this arises because of the relatively dense PCM has smaller pores, reducing collagen realignment, strain-stiffening and long-range force transmission.

These simulation results are of interest in the context of mesenchymal development, whereby cells in many solid tissues transition from receiving extensive signals from neighboring cells early in development to becoming more insulated by ECM and PCM later in development (Cosgrove et al., 2016; Vining and Mooney, 2017; Zhang et al., 2022). Mechanical signals from neighboring cells can further pathologies such as fibrosis (Liu et al., 2020). Results indicate that the fibrous structure of the ECM, which exhibits stretch stiffening and long-range force transmission, enhances mechanosensing of neighboring cells, but that the development of the PCM subsequently diminishes this. Thus, the mechanical and geometric properties of the PCM and cell microenvironment are factors that can be tuned to accentuate or attenuate cell-cell mechanosensing.

3.5. PCM shields cells from external mechanical stretch

To assess how the PCM affects transduction of exogenous stretching of a tissue, we tested the hypothesis that a fibrous PCM shields cells from far-field stretch by exploring uniaxial stretch of 3D fibrous and neoHookean systems (Fig. 6). To quantify the effect of the PCM, we defined the Taylor deformation parameter D as:

$$D = \frac{\lambda_z^{cell} h - \lambda_\perp^{cell} R_0}{\lambda_z^{cell} h + \lambda_\perp^{cell} R_0} \tag{9}$$

A large Taylor deformation parameter D means large elongation of the cell. Although cells are poroelastic (Peng et al., 2020a, 2020b) and can exchange water and ions with their environment (Alisafaei et al., 2019; Peng et al., 2022a, 2022b), these exchanges take minutes to hours (Liu et al., 2019). We therefore simulated cases in which cell volume remained constant during deformation.

We applied a far-field stress σ_r to the ECM (Fig. 6e) and calculated the Taylor deformation parameter D of cells with or without PCM. With increasing stress, cells elongated monotonically in a fibrous ECM (Fig. 6a). As the PCM became thicker, but with material properties unchanged, cell morphology changed less with increasing stress, indicating that thicker PCM shielded cells from external stress.

For cells embedded inside neoHookean ECM and PCM, similar trends were observed. However, for the same PCM thickness, a cell within neoHookean ECM stretched more (Fig. 6b). This was due to the strain-stiffening of fibrous ECM: fibrous material becomes more difficult to distend with increasing stressσ_r, resulting in the Taylor deformation parameter D versus far-field stress σ_r curve being a convex function (Fig. 6a). However, the hyperelastic, neoHookean ECM lacks strain stiffening property, leading to a more elongated cell shape (Fig. 6b).

We further investigated the effects of the other two fibrous material parameters, the fiber stiffness $\chi_m = E_{fECM}/E_{ECM}$ and the fiber strain-hardening ratio m, to assess the role of PCM strain-stiffening on cell shielding. As the fiber stiffness χ_m increased, cell elongation at the same far-field stress σ_r decreased. This phenomenon became more obvious as far-field stress increased. This occurred because, with smaller external stress, the isotropic part of the collagen network dominated, and the curves were thus closer to each other (Fig. 6c). When the external stress σ_r became larger, the collagen realigned and the nonlinear stiffening began to dominate. This stiffening along the principal strain direction increased with fiber stiffness χ_m, leading to reduced distortion of the cell (Fig. 6c). A similar trend was found when changing the fiber strain-hardening ratio m, with differences between curves for different m increasing evident with increasing far-field stress σ_r (Fig. 6d). Although in both cases, higher tension leads to greater collagen network stiffening, the cell response was more sensitive to fiber stiffness χ_m than to fiber strain-hardening ratio m.

3.6. Normalized PCM stiffness plays a dominant role in strain shielding

As cells such as chondrocytes develop, they recruit an increasingly stiff PCM region around them (Wilusz et al., 2014). To assess the effect of this PCM stiffening on strain-shielding, we loaded the model of Fig. 6 to a constant value of far-field stress, $\sigma_r/G_m = 0.5$, and studied the effect of normalized PCM stiffness E_{PCM}/E_{ECM} (Fig. 7). In a fibrous ECM, the Taylor deformation parameter D decreased monotonically with increasing PCM stiffness, as expected for cells inside a stiffer shell (Fig. 7a). Increasing PCM thickness in general increased strain shielding (Fig. 7a), with thicker PCM bearing more of the loading. Effects of PCM thickness were negligible both for E_{PCM}/E_{ECM} near unity, and for a relatively rigid PCM ($E_{PCM}/E_{ECM} \sim 1000$) (Fig. 7a).

Similar trends were observed in a neoHookean system (Fig. 7b), although cell deformation was substantially higher in the neo-Hookean system. For instance, when $E_{PCM}/E_{ECM} \sim 1$, the Taylor deformation parameter D in Fig. 7b is almost three times larger than the value in Fig. 7a. This is again because of the strain-stiffening of the collagen network that is superimposed upon the hyperelastic, isotropic background. Strain-stiffening in the collagen network offloads stress from the cell, possibly affording it protection from excess loading.

We next assessed the effects of fiber stiffness χ_m and fiber strain-hardening ratio m on strain shielding for cells embedded in PCM of different stiffnesses. Here, the greatest effects were observed for lower values of E_{PCM}/E_{ECM}. As χ_m increased, the Taylor deformation parameter D decreased (Fig. 7c). The strong effect of χ_m at $E_{PCM}/E_{ECM} \sim 1$ is at first surprising because no mismatch in background modulus exists, but can be explained by the dominant role of fiber strain-stiffening on strain shielding. The effect of χ_m diminished with increasing PCM stiffness, and was less than 1% for $E_{PCM}/E_{ECM} > 30$. This is because the PCM stretch drops to the point that strain stiffening no longer is a factor in the PCM's behavior. Similar trends are observed for the strain stiffening exponent, m (Fig. 7d).

4. Conclusions

The fibrous ECM and PCM serve many physiological roles, including roles that preclude the use of a non-fibrous elastic matrix, such as serving as a porous scaffold to enable the exchange of metabolites with the extracellular environment. The fibrous ECM has previously been shown to have additional features that are useful for development and wound healing, specifically a strain-stiffening feature that enables transduction of mechanical loads by cells during development and wound healing, and that triggers a recursive dialog between cells and ECM (Wilusz et al., 2014). However, for cells in a collagenous matrix, this recursive dialog drives the accumulation of local PCM that changes the mechanical microenvironment. This study revealed a range of ways in which the fibrous character of the PCM affects the mechanical microenvironment of cells.

The same factors that enable long-range transmission of mechanical signals by cells eventually serve to isolate them. This long-range transmission arises from collagenous ECM that dominates structural tissues and has unique structural properties that enable it to stiffen under external straining. Results from the current work suggest that this strain-stiffening, especially in the PCM, serves to maintain cell morphology but weaken the transmission of force and the mutual communication between cells. However, the cells themselves polarize as the PCM develops, and results show that the more concentrated stress at the poles that arises through polarization of either shape or contractile polarization harnesses the fibrous properties of PCM to overcome this shielding of long-range force transmission. These strain stiffening features of the fibrous PCM resist external force or deformation, possibly shielding cells from excessive stretch known to disrupt stress fibers (Lee et al., 2012) or injure cells (Ellis et al., 1995; McKinney et al., 1996).

Feedback between cells and ECM is known to be sensitive to the stiffness of the surrounding matrix, with both cell contractility and nuclear mechanics being sensitive to the mechanical fields transmitted by the matrix (Hall et al., 2016; Ronan et al., 2014). This adds a layer of complexity to the force transmission through the PCM and ECM. Because the active stress produced by a cell typically increases with the stiffness of the ECM up to a saturation point, cells within a stiffer PCM may generate greater contractility that could potentially

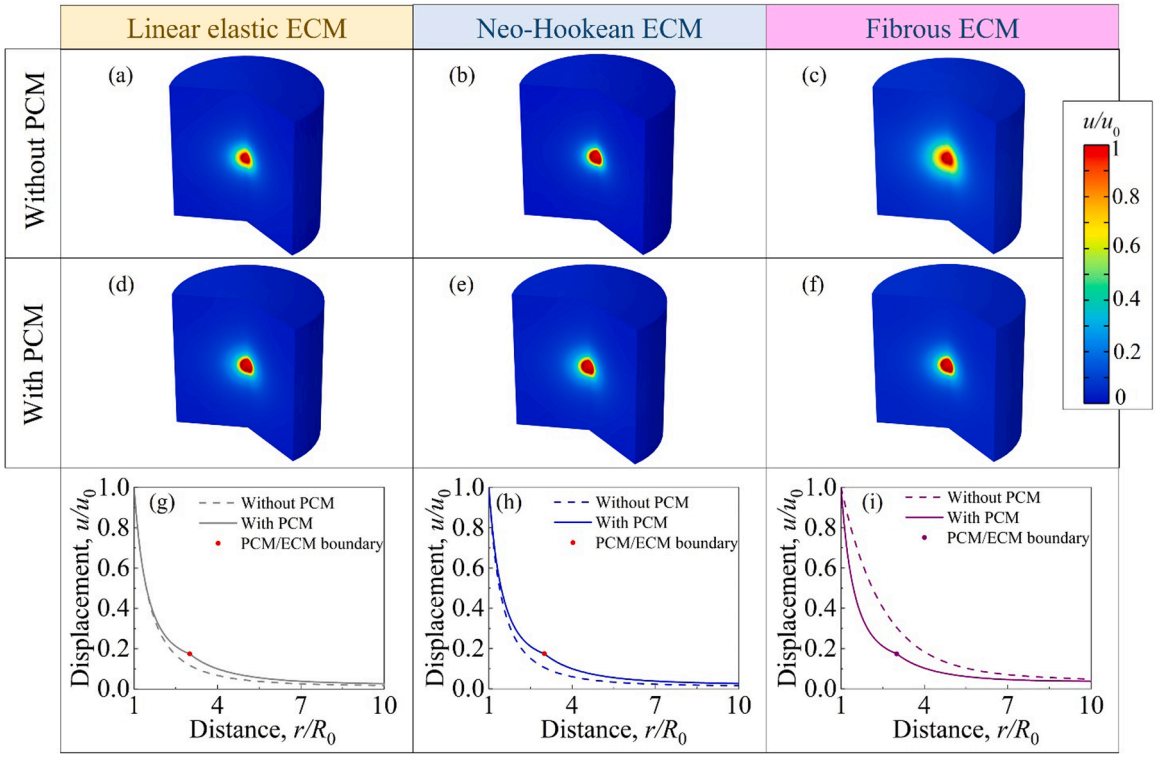

Fig. A1. The effect of PCM on displacement fields in 3D linear elastic, neoHookean, and fibrous ECMs when subjected to spherical and isotropic contraction from a cell. (a-c) Contour plots of normalized displacement fields due to cell contraction in systems with no PCM. (d-f) Contour plots illustrating the normalized displacement fields due to cell contraction in systems containing PCM. (g–i) Normalized displacement fields within the midplane of the cylinder. Parameters for all plots: inward normal traction = 0.4 kPa, E_{ECM}=2 kPa, E_{PCM}/E_{ECM}=100, Poisson's ratio $\nu = 0.3$; additionally, for the fibrous ECM: fiber stiffness $\chi_m = E_{fECM}/E_{ECM}$ =50, fiber strain-hardening exponent $m = 30$, critical stretch $\lambda_c = 1.001$. The thickness of the PCM was set to be $t = 2R_0$.

compensate for otherwise attenuated force transmission. However, in cases where the PCM is excessively dense, such as in fibrotic disease, the cell's saturation point for contractility may be reached. Consequently, the stress and displacement fields within the PCM may become attenuated, hindering cell-cell mechanical communication beyond a threshold of PCM stiffness.

In this study, both ECM and PCM were modeled with a constitutive law that is appropriate for collagen. ECM and PCM are in fact more complex, containing a range of molecules such as proteoglycans, fibronectins, and elastin (Chen et al., 2022). The current results lay only a foundation for understanding how these factors within the PCM affect cell mechanotransduction and behavior. Of particular interest may be how additional PCM components affect the balance between a weakening of mechanical and cell-cell communication on the one hand, known to be essential for development and homeostasis (Wilusz et al., 2014), and on the other a strengthening of strain-shielding, known to be protective in fibrocartilage (Han et al., 2016). Additionally, these additional ECM and PCM components may affect how cell polarity can achieve long-range force transmission through a fibrous PCM. These factors are all controlled to some degree by local remodeling of both cell and PCM architecture by a cell and point to microenvironmental factors that can be tailored both physiologically and pathophysiologically.

Declaration of Competing Interest

The authors declare that they have no known competing financial interests or personal relationships that could have appeared to influence the work reported in this paper.

Data availability

Data will be made available on request.

Acknowledgments

This work was supported by the NSF through the NSF Science and Technology Center for Engineering Mechanobiology (grant

CMMI 1548571), grant DMR-2105150, and grant OIA-2219142, and by the NIH through grants R01AR077793, R01HL159094, and R01DK131177.

Appendix

To study the impact of the PCM on stress transmission, we modeled cell contractility as a uniform, inward active traction applied normal to the inner boundary of the PCM. The normal traction field had a magnitude of 0.4 kPa (Zahalak et al., 2000). The simulations were otherwise identical to those in which displacement fields were instead applied to the inner boundary of the PCM. The trends observed were analogous to those observed in the latter (Fig. A1).

References

Ahmadzadeh, H., Webster, M.R., Behera, R., Valencia, A.M.J., Wirtz, D., Weeraratna, A.T., Shenoy, V.B., 2017. Modeling the two-way feedback between contractility and matrix realignment reveals a nonlinear mode of cancer cell invasion. Proc. Natl Acad. Sci. 114, E1617–E1626.

Alexopoulos, L.G., Setton, L.A., Guilak, F., 2005. The biomechanical role of the chondrocyte pericellular matrix in articular cartilage. Acta Biomater. 1, 317–325.

Alisafaei, F., Chen, X., Leahy, T., Janmey, P.A., Shenoy, V.B., 2021. Long-range mechanical signaling in biological systems. Soft Matter 17, 241–253.

Alisafaei, F., Jokhun, D.S., Shivashankar, G.V., Shenoy, V.B., 2019. Regulation of nuclear architecture, mechanics, and nucleocytoplasmic shuttling of epigenetic factors by cell geometric constraints. Proc. Natl Acad. Sci. 116, 13200–13209.

Alisafaei, F., Moheimani, H., Elson, E.L., Genin, G.M., 2023. A nuclear basis for mechanointelligence in cells. Proc. Natl Acad. Sci. 120, e2303569120.

Alisafaei, F., Shakiba, D., Iannucci, L.E., Davidson, M.D., Pryse, K.M., Chao, P.-h.G., Burdick, J.A., Lake, S.P., Elson, E.L., Shenoy, V.B., 2022. Tension Anisotropy Drives Phenotypic Transitions of Cells Via Two-Way cell-ECM Feedback. bioRxiv, 2022. 2003. 2013.484154.

Babaei, B., Davarian, A., Lee, S.L., Pryse, K.M., McConnaughey, W.B., Elson, E.L., Genin, G.M., 2016. Remodeling by fibroblasts alters the rate-dependent mechanical properties of collagen. Acta Biomater. 37, 28–37.

Babaei, B., Velasquez-Mao, A.J., Thomopoulos, S., Elson, E.L., Abramowitch, S.D., Genin, G.M., 2017. Discrete quasi-linear viscoelastic damping analysis of connective tissues, and the biomechanics of stretching. J. Mech. Behav. Biomed. Mater. 69, 193–202.

Ban, E., Franklin, J.M., Nam, S., Smith, L.R., Wang, H., Wells, R.G., Chaudhuri, O., Liphardt, J.T., Shenoy, V.B., 2018. Mechanisms of plastic deformation in collagen networks induced by cellular forces. Biophys. J. 114, 450–461.

Bonfoh, N., Hounkpati, V., Sabar, H., 2012. New micromechanical approach of the coated inclusion problem: exact solution and applications. Comput. Mater. Sci. 62, 175–183.

Chen, X., Chen, D., Ban, E., Toussaint, K.C., Janmey, P.A., Wells, R.G., Shenoy, V.B., 2022. Glycosaminoglycans modulate long-range mechanical communication between cells in collagen networks. Proc. Natl Acad. Sci. 119, e2116718119.

Cosgrove, B.D., Mui, K.L., Driscoll, T.P., Caliari, S.R., Mehta, K.D., Assoian, R.K., Burdick, J.A., Mauck, R.L., 2016. N-cadherin adhesive interactions modulate matrix mechanosensing and fate commitment of mesenchymal stem cells. Nat. Mater. 15, 1297–1306.

Deogekar, S., Picu, R., 2018. On the strength of random fiber networks. J. Mech. Phys. Solids 116, 1–16.

Dowling, E.P., Ronan, W., McGarry, J.P., 2013. Computational investigation of *in situ* chondrocyte deformation and actin cytoskeleton remodelling under physiological loading. Acta Biomater. 9, 5943–5955.

Doyle, A.D., Carvajal, N., Jin, A., Matsumoto, K., Yamada, K.M., 2015. Local 3D matrix microenvironment regulates cell migration through spatiotemporal dynamics of contractility-dependent adhesions. Nat. Commun. 6, 1–15.

Ellis, E.F., McKinney, J.S., Willoughby, K.A., Liang, S., Povlishock, J.T., 1995. A new model for rapid stretch-induced injury of cells in culture: characterization of the model using astrocytes. J. Neurotrauma 12, 325–339.

Fang, F., Sawhney, A.S., Lake, S.P., 2014. Different regions of bovine deep digital flexor tendon exhibit distinct elastic, but not viscous, mechanical properties under both compression and shear loading. J. Biomech. 47, 2869–2877.

Fraley, S.I., Wu, P.-h., He, L., Feng, Y., Krisnamurthy, R., Longmore, G.D., Wirtz, D., 2015. Three-dimensional matrix fiber alignment modulates cell migration and MT1-MMP utility by spatially and temporally directing protrusions. Sci. Rep. 5, 1–13.

Genin, G.M., Kent, A., Birman, V., Wopenka, B., Pasteris, J.D., Marquez, P.J., Thomopoulos, S., 2009. Functional grading of mineral and collagen in the attachment of tendon to bone. Biophys. J. 97, 976–985.

Hall, M.S., Alisafaei, F., Ban, E., Feng, X., Hui, C.Y., Shenoy, V.B., Wu, M., 2016. Fibrous nonlinear elasticity enables positive mechanical feedback between cells and ECMs. Proc. Natl Acad. Sci. 113, 14043–14048.

Han, W.M., Heo, S.J., Driscoll, T.P., Delucca, J.F., McLeod, C.M., Smith, L.J., Duncan, R.L., Mauck, R.L., Elliott, D.M., 2016. Microstructural heterogeneity directs micromechanics and mechanobiology in native and engineered fibrocartilage. Nat. Mater. 15, 477–484.

Han, WM., Heo, S.J., Driscoll, TP., Smith, LJ., Mauck, RL., Elliott, DM., 2013. Macro- to microscale strain transfer in fibrous tissues is heterogeneous and tissue-specific. Biophys. J. 105, 807–817.

Han, Y.L., Ronceray, P., Xu, G., Malandrino, A., Kamm, R.D., Lenz, M., Broedersz, C.P., Guo, M., 2018. Cell contraction induces long-ranged stress stiffening in the extracellular matrix. Proc. Natl Acad. Sci. 115, 4075–4080.

Hong, Y., Peng, X., Yu, H., Jafari, M., Shakiba, D., Huang, Y., Qu, C., Melika, E.E., Tawadros, A.K., Mujahid, A., 2022. Mechanobiology of Fibroblast Activation in Skin Grafting. bioRxiv, 2022.2010. 2012.511903.

Huang, G., Li, F., Zhao, X., Ma, Y., Li, Y., Lin, M., Jin, G., Lu, T.J., Genin, G.M., Xu, F., 2017. Functional and biomimetic materials for engineering of the three-dimensional cell microenvironment. Chem. Rev. 117, 12764–12850.

Lee, S.L., Nekouzadeh, A., Butler, B., Pryse, K.M., McConnaughey, W.B., Nathan, A.C., Legant, W.R., Schaefer, P.M., Pless, R.B., Elson, E.L., Genin, G.M., 2012. Physically-induced cytoskeleton remodeling of cells in three-dimensional culture. PLoS One 7, e45512.

Liu, L., Yu, H., Zhao, H., Wu, Z., Long, Y., Zhang, J., Yan, X., You, Z., Zhou, L., Xia, T., Shi, Y., Xiao, B., Wang, Y., Huang, C., Du, Y., 2020. Matrix-transmitted paratensile signaling enables myofibroblast–fibroblast cross talk in fibrosis expansion. Proc. Natl Acad. Sci. 117, 10832–10838.

Liu, S., Tao, R., Wang, M., Tian, J., Genin, G.M., Lu, T.J., Xu, F., 2019. Regulation of cell behavior by hydrostatic pressure. Appl. Mech. Rev. 71, 0408031–4080313.

Long, Y., Niu, Y., Liang, K., Du, Y., 2022. Mechanical communication in fibrosis progression. Trends Cell Biol. 32, 70–90.

McKinney, J.S., Willoughby, K.A., Liang, S., Ellis, E.F., 1996. Stretch-induced injury of cultured neuronal, glial, and endothelial cells. Stroke 27, 934–940.

Nerurkar, N.L., Baker, B.M., Sen, S., Wible, E.E., Elliott, D.M., Mauck, R.L., 2009. Nanofibrous biologic laminates replicate the form and function of the annulus fibrosus. Nat. Mater. 8, 986–992.

Peng, X., He, W., Xin, F., Genin, G.M., Lu, T.J., 2020a. The acoustic radiation force of a focused ultrasound beam on a suspended eukaryotic cell. Ultrasonics 108, 106205. Ultrasonics.

Peng, X., He, W., Xin, F., Genin, G.M., Lu, T.J., 2020b. Standing surface acoustic waves, and the mechanics of acoustic tweezer manipulation of eukaryotic cells. J. Mech. Phys. Solids 145, 104134.

Peng, X., He, W., Xin, F., Genin, G.M., Lu, T.J., 2021. Effects of coating on dynamic stress concentration in fiber reinforced composites. Int. J. Solids Struct. 222-223, 111029.

Peng, X., Huang, Y., Alisafaei, F., 2022a. Cytoskeleton-mediated alterations of nuclear mechanics by extracellular mechanical signals. Biophys. J. 121, 1–3.
Peng, X., Liu, Y., He, W., Hoppe, E.D., Zhou, L., Xin, F., Haswell, E.S., Pickard, B.G., Genin, G.M., Lu, T.J., 2022b. Acoustic radiation force on a long cylinder, and potential sound transduction by tomato trichomes. Biophys. J. 121, 3917–3926.
Picu, R., 2011. Mechanics of random fiber networks—A review. Soft Matter 7, 6768–6785.
Rashid, F., Liu, W., Wang, Q., Ji, B., Irudayaraj, J., Wang, N., 2023. Mechanomemory in protein diffusivity of chromatin and nucleoplasm after force cessation. Proc. Natl Acad. Sci. 120, e2221432120.
Reynolds, N., McEvoy, E., Ghosh, S., Panadero Pérez, J.A., Neu, C.P., McGarry, P., 2021. Image-derived modeling of nucleus strain amplification associated with chromatin heterogeneity. Biophys. J. 120, 1323–1332.
Romani, P., Valcarcel-Jimenez, L., Frezza, C., Dupont, S., 2021. Crosstalk between mechanotransduction and metabolism. Nat. Rev. Mol. Cell Biol. 22, 22–38.
Ronan, W., Deshpande, V.S., McMeeking, R.M., McGarry, J.P., 2014. Cellular contractility and substrate elasticity: a numerical investigation of the actin cytoskeleton and cell adhesion. Biomech. Model Mechanobiol. 13, 417–435.
Saraswathibhatla, A., Indana, D., Chaudhuri, O., 2023. Cell–Extracellular Matrix Mechanotransduction in 3D. Nature Reviews Molecular Cell Biology.
Seo, B.R., Chen, X., Ling, L., Song, Y.H., Shimpi, A.A., Choi, S., Gonzalez, J., Sapudom, J., Wang, K., Andresen Eguiluz, R.C., 2020. Collagen microarchitecture mechanically controls myofibroblast differentiation. Proc. Natl Acad. Sci. 117, 11387–11398.
Shakiba, D., Alisafaei, F., Savadipour, A., Rowe, R.A., Liu, Z., Pryse, K.M., Shenoy, V.B., Elson, E.L., Genin, G.M., 2020. The balance between actomyosin contractility and microtubule polymerization regulates hierarchical protrusions that govern efficient fibroblast–collagen interactions. ACS Nano 14, 7868–7879.
Siadat, S.M., Ruberti, J.W., 2023. Mechanochemistry of collagen. Acta Biomater. 163, 50–62.
Vining, K.H., Mooney, D.J., 2017. Mechanical forces direct stem cell behaviour in development and regeneration. Nat. Rev. Mol. Cell Biol. 18, 728–742.
Wang, H., Abhilash, A.S., Chen, CS., Wells, RG., Shenoy, VB., 2014. Long-range force transmission in fibrous matrices enabled by tension-driven alignment of fibers. Biophys. J. 107, 2592–2603.
Wilusz, R.E., Sanchez-Adams, J., Guilak, F., 2014. The structure and function of the pericellular matrix of articular cartilage. Matrix Biol. 39, 25–32.
Zahalak, G.I., Wagenseil, J.E., Wakatsuki, T., Elson, E.L., 2000. A cell-based constitutive relation for bio-artificial tissues. Biophys. J. 79, 2369–2381.
Zhang, Z., Sha, B., Zhao, L., Zhang, H., Feng, J., Zhang, C., Sun, L., Luo, M., Gao, B., Guo, H., Wang, Z., Xu, F., Lu, T.J., Genin, G.M., Lin, M., 2022. Programmable integrin and N-cadherin adhesive interactions modulate mechanosensing of mesenchymal stem cells by cofilin phosphorylation. Nat. Commun. 13, 6854.